Operational Experience with the Emittance-Meter at SPARC*

L. Catani†, A. Cianchi, INFN-Roma Tor Vergata, Roma, Italy
C. Ronsivalle, ENEA C.R. Frascati, Roma, Italy
P. Musumeci, M. Petrarca, INFN-Roma, Roma, Italy
M. Bellaveglia, R. Boni, M. Boscolo, M. Castellano, E. Chiadroni, L. Cultrera,
G. Di Pirro, A. Drago, M. Ferrario, D. Filippetto, V. Fusco, A. Gallo, G. Gatti,
F. Tazzioli, C. Vaccarezza, M. Vescovi, C. Vicario, INFN-LNF, Frascati, Roma, Italy
M. Migliorati, L. Palumbo, University La Sapienza, Roma, Italy.

Abstract

We report the operational experience of the movable emittance meter at SPARC. It is based on the well-known technique of pepper pot measurements (1-D slits in our case) but, in addition, it allows moving the measuring device along the beam line from about 840 mm to 2200 mm from the cathode, following the emittance oscillations. More than a simple improvement over conventional, though non-trivial, beam diagnostic tools this device defines a new strategy for the characterization of high performance photo-injectors, providing a tool for detailed analysis of the beam dynamics, over a section of the accelerator where emittance compensation take place. With this device we planned to perform detailed and systematic studies on beam dynamics with particular attention to the transverse parameters as well as longitudinal.

INTRODUCTION

The aim of the SPARC [1] project is to promote R&D towards high brightness photo-injectors to drive a SASE-FEL experiment. The 150 MeV SPARC photo-injector consists of a 1.6 cell RF gun operated at S-band (2.856 GHz, of the BNL/UCLA/SLAC type) and high-peak field on the cathode incorporated metallic photo-cathode of 120 MV/m, generating a 5.6 MeV, 100 A (1 nC, 10 ps) beam.

The beam is then focused and matched into 3 SLAC-type accelerating sections, which boost its energy to 150-200 MeV. The first phase of the SPARC Project was dedicated to the beam RMS emittance measurement along the drift space following the RF gun, where the emittance compensation process occurs.

The complete characterization of the beam parameters at different distances from the cathode is important to define the injector settings optimizing emittance compensation and for code validation. For this measurement, a dedicated moveable (in z, z being the distance from the cathode, measured along the accelerator axis) emittance measurement device [3] (emittance-meter) is used allowing to measure the RMS emittance in the range from about z=86 cm to z=210 cm.

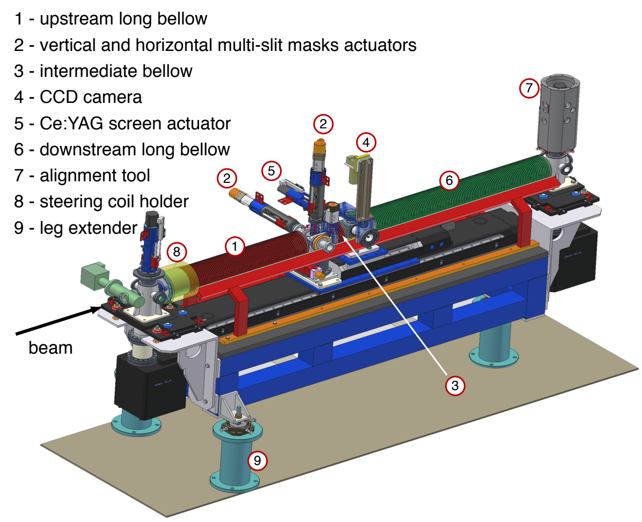

Figure 1: 3D mechanical drawing of the SPARC emittance-meter

The technique to measure the beam emittance and the phase space, in both the horizontal and vertical planes, makes use of a double system of horizontal and vertical slit masks [2]. Each mask consists of a slits array (7 slits, 50 μm width spaced of 500 μm, 2 mm thick) and two single slits, 50 and 100 μm width. The slits are realized by photo-chemical etching providing, compared to mechanical machining, higher precision and improved smoothness of slits edges. The multislits are used for single shot measurements, provided the beam size is large enough for an adequate beam sampling by the slit array. Alternatively, a single slit can be moved across the beam spot. In this case the accuracy of transverse sampling can be freely chosen adjusting the step between the different positions of the slit. This measurement is an integration over many pulses.

Linear actuators with stepper motors are used to control the insertion of the slits masks into the beamline. A differential encoder and a reference end switch guarantee reproducibility and accuracy of the movement to better than 2 μm, required for single-slit multi-shots measurements.

The projected cross-section of beamlets emerging from the slit-mask are measured by means of a downstream

* This work has been partially supported by the EU Commission in the sixth framework program, contract no. 011935 EUROFEL-DS1.
† luciano.catani@roma2.infn.it

Ce:YAG radiator. Because beam size and divergence depend on the longitudinal position, the slit to screen distance must be properly adjusted in order to optimize the accuracy of the beamlets profile measurement as the movable device is placed at different z. A bellow is therefore interposed between the slit mask and the screen, allowing their relative distance to be changed while keeping the masks at a fixed position with respect to the gun. This solution allows to set the length of drift between slit mask and the screen that best fits the different scenarios: converging beam, diverging beam, single or multi-slits. Refer to Fig.1 for a schematic drawing of the emittance meter.

Radiation emitted in the forward direction from the Ce:YAG crystal is collected by a 45 degrees mirror downstream from the radiator. The back face of the transparent crystal radiator is observed, thus minimizing degradation of the spatial resolution due to the depth of field of the optics.

Beam images are acquired using digital CCD cameras equipped with a 105mm ”macro” type objective. The magnification of 0.66 gives a resolution of 15.4 μm per pixel.

Beam charge is measured by means of a Faraday cup, placed in a cross together with a chrome-oxide screen to image the beam at 60 cm from the cathode. This screen is also used to monitor the position of the laser spot on the cathode. The emittance-meter is followed by a magnetic spectrometer measuring the beam energy and energy spread

DETAILS ON MEASUREMENTS WITH THE MOVABLE EMITTANCE-METER

The movable emittance-meter was built to perform a detailed characterization of the SPARC photo-injector studying the beam dynamics as function of relevant parameters such as the solenoid field, the beam charge and size, the laser pulse length and its shape. Refer to [4] for more details.

Beam Envelope

Evolution of the bunch transverse size along the photo-injector is a important, though simple, measurement we regularly perform with the emittance-meter. It takes less than 5 minutes to complete the measurement consisting of continuously changing the z-position of the movable system between the upper and lower ends to grabb beam images at various position. These images are on-line processed to filter out the background noise and to calculate the RMS value of the beam size. In Fig.2 are shown results of measurements of the RMS beam size vs z for different values of the solenoid field at the gun. The measurement procedure is a completely automatic one-click operation of the control system.

At a glance we can guess the solenoid current that gives the waist in the required z position or, by comparing x and y envelopes curves, check for the causes that might produce beam envelope irregularities, laser or solenoid misalignment for instance. The different curves in Fig.2 show how the beam waist and its position in z are changed as consequence of the different solenoid currents.

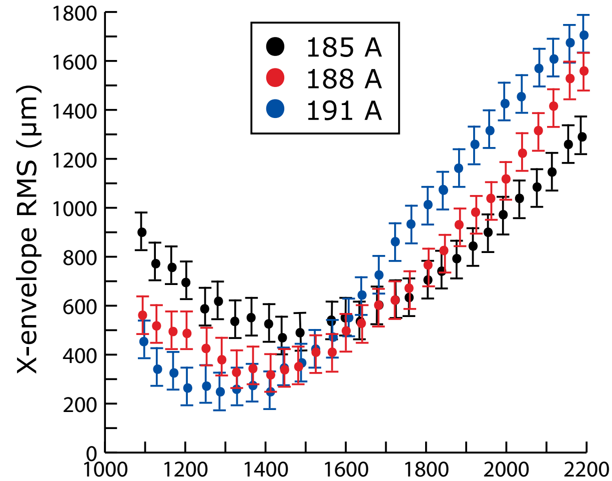

Figure 2: Envelope of the beam (x-plane) along z for different solenoid currents

Emittance

The emittance can be measured, in both x and y planes, at different positions along the emittance-meter. The beam size and its divergence are expected to change as the distance from the cathode changes: the beam is converging at the beginning of the emittance-meter and diverging in the second half. Different measurement strategies are then implemented to achieve the best accuracy of the emittance calculation algorithm.

When the beam is close to the waist, its size is small and the multi-slits mask is not suited because it produces a limited number of beamlets. The single-slits multi-shot measurement is also preferable in the region close to the end of the emittance-meter where the beam size is typically larger than the part of the mask covered by the slit-array and when the beam is strongly converging because profiles of beamlets produced by the multi-slits mask might overlap. Typical values of the sampling distance between the slit positions ranges from 110 μm to 380 μm. At least nine beamlets are always collected with the single slit. In all of the other conditions the multi-slits mask provides fast single-shot measurements, while the single-slit is preferred for accurate analysis.

It’s worth mentioning that, for given beam conditions, results produced by both single-slit and multi-slit measurement have always been fully consistent. A simple check of results produced by the emittance calculation algorithm consists in comparing the RMS beam size at the slit-mask (measured by moving the screen at the longitudinal position of the slit-mask during emittance measurement) against the value of beam size estimated by the emittance calculation algorithm. We always obtained an excellent agreement between the two results.

Fig.3 shows an example of emittance measurements at different positions along the emittance-meter. In this case the beam charge was 700 pC and the energy 5.14 MeV with a longitudinal profile σ= 4.35 psec.

A typical emittance measurement with the single-slit mask consists of collecting 15 beam images for each slit position. The center of mass and RMS size of beamlets are calculated for each image and averaged. We verified that larger statistic doesn't significantly improve the accuracy of results. In details, from each beamlets image we calculate the projection on the axis, subtract the baseline, try gaussian fit to find the best position for the center of intensity distribution, reduce the number of the relevant points skipping these that are outside the 3 standard deviations from the centre and only on the remaining points we calculate the RMS parameters.

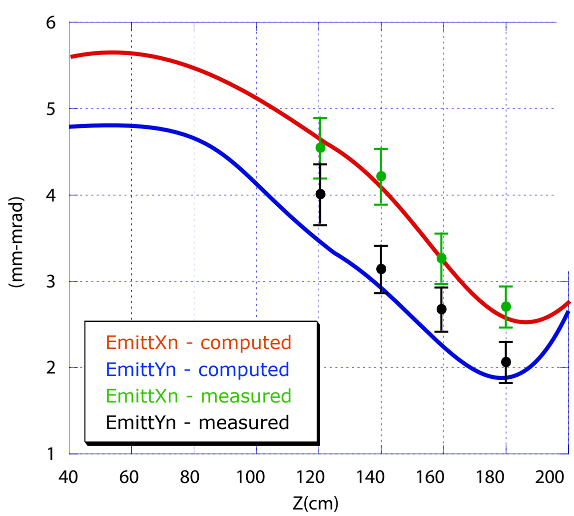

Figure 3: Emittance measurements along the e-meter

The high magnification optical system, the high efficiency YAG screen and a CCD with a remotely controlled gain always provide a good signal to noise ratio and large number of sampling point for every beamlet in all the conditions.

Transverse phase space

The measurement of RMS Twiss parameters and emittance with the single-slit mask allow, as a side-product, the reconstruction of the beam transverse phase space [5]. For each slit position, the beamlet profile on the screen yelds the divergence distribution of particles at the given x position, i.e. those emerging from the slit-mask. Interpolation of the different profiles produces the two dimensional x - x' distribution.

In Fig.4 we show the phase-space measured at different positions along the emittance-meter for a low charge (100 pC) beam. Clearly the beam is going through a focus evolving from convergent to divergent. On the other hand, as the photoinjector theory predicts, the evolution has many differences from that in a linear optics crossover. In a "standard" drift the particles being on the left (negative x) move to the right crossing the origin thus following the lines of motion of constant x. Here the particles that are on left at the beginning of the beamline stay on the left. They get close to the origin (both in x and x') without crossing it and after the laminar space charge dominated waist they move back (still negative x) changing the sign of their divergence

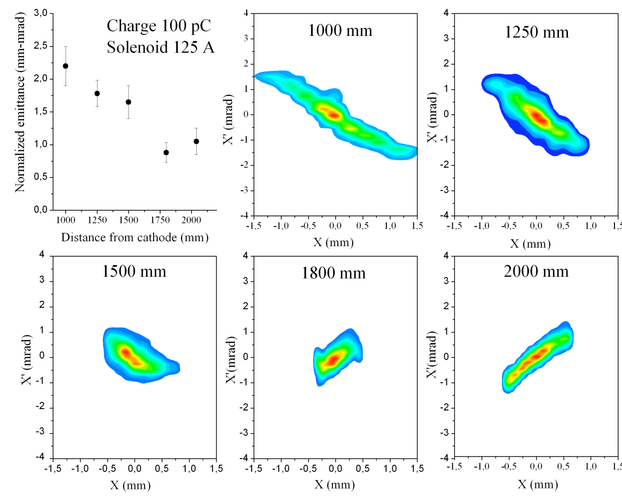

Figure 4: Phase space measure along the e-meter

subsectionBeam energy and energy spread

The e-meter gives also the possibility to investigate the longitudinal dynamics and correlation between transverse and longitudinal planes.

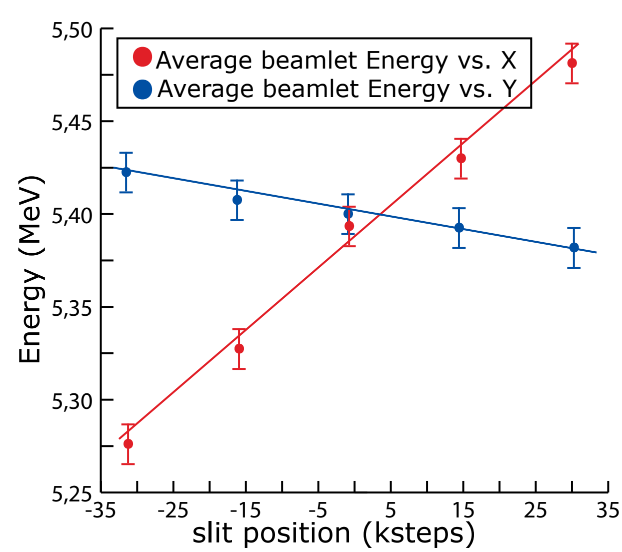

Figure 5: Beamlet energy vs transverse position

Moving the x or y single-slit across the beam and measuring the energy at the spectrometer gives evidence of a possible correlation between particles transverse position and their energy. The measurements in Fig.5 show a variation of beamlets mean energy when the position of the vertical single-slit is changed moving it across the beam in the horizontal direction. The correlation, clearly stronger in the x-direction, suggest as possible cause the non-normal incidence of the laser beam on the cathode in the y=0 plane.

As a final example of the extended diagnostic capabilities of the emittance-meter we report in Fig.6 the evolution of the energy spread measured for the central beamlet (i.e. with the vertical single-slit centered on the beam center of mass) as function of the position along z of the slit mask.

Note that all the points in the graph, except the last one representing the energy spread of the whole beam obtained removing the slit-mask from the beam path, correspond to positions within the high impedance bellows. Inside the long bellows the wakefields contribution to the energy spread adds to the longitudinal space charge effect and the energy spread grows faster. These effects significantly contribute to the energy spread up to the slit-mask while for the low charge beamlet the wakefields and space charge effect are practically negligible. As consequence an increasing energy spread is expected as the distance of the slit-mask from the cathode became larger. It is clearly confirmed by

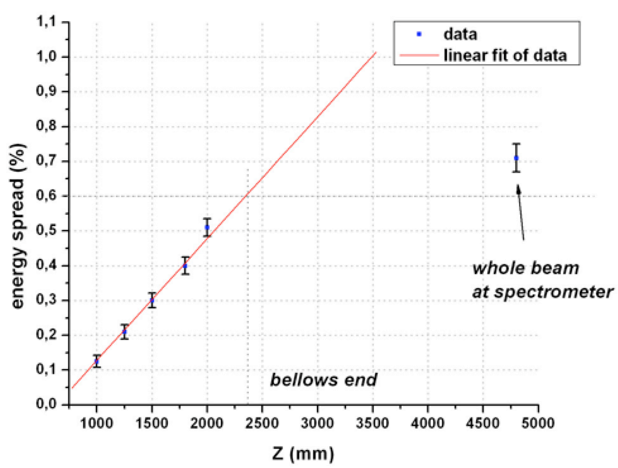

Figure 6: Contribution of bellows to energy spread is evidenced selecting a small portion of the beam with the singl-slit mask and moving it at different Z.

CONCLUSION

The final task of the SPARC photo-injector commissioning is to provide a complete sets of measurements (including transverse and longitudinal profiles of the laser) allowing a complete characterization of the beam dynamics by following the evolution of all the beam parameters.

As it appears from the previous paragraphs, beam dynamics in a photo-injector is a non trivial problem that critically depends on many variables. In systems equipped with a single (at a given longitudinal position) emittance diagnostic station, beamline parameters like solenoid strength or laser launching phase are varied to obtain emittance values that can be checked against those predicted by simulation codes. Unfortunately, the changing of a set-point is often hindering a cross-talk between different simulation parameters which so far has been taken into account somewhat externally (for example varying the gun phase affects the extracted charge, and varying the solenoid strength changes the quadrupole component effect).

The clear advantage in characterizing a photo-injector with the SPARC movable emittance-meter is that once the working point is set, a single simulation run generates results which reproduce the evolution of the experimental data (beamsize, emittance, energy spread) taken with the movable measurement device at the different positions along the beamline. In other words a single simulation run can be checked against a number of experimental points, not just a single one, all representing, or measured with, the same identical photo-injector working point.

Further work, more detailed and accurate measurements, is foreseen in order to approach such ambitious goal, fully understand the system, and validate the prediction capabilities of the modeling codes.

REFERENCES

[1] D. Alesini et al., Nucl. Instr. & Meth. In Phys. Res. A 507 (2003) 345-349C.

[2] M. Zhang, FERMILAB-TM-1988, Oct 1996.

[3] L.Catani et.al., Rev. Sci. Instrum. 77, 093301 (2006).

[4] M. Bellaveglia ”Commissioning of SPARC Photoinjector”, these Proceedings.

[5] S. G. Anderson et al. ”Space-charge effects in high brightness electron beam emittance measurements”, Phys. Rev. ST Accel. Beams 5, 014201 (2002).